Isospin effects in $\pi^{\pm}$ elastic scattering from ^{12}C, ^{13}C, and ^{14}C at 65 and 80 MeV

M. Blecher and K. Gotow
Virginia Polytechnic Institute and State University, Blacksburg, Virginia 24061

R. L. Burman, M. V. Hynes, and M. J. Leitch
Los Alamos National Laboratory, Los Alamos, New Mexico 87545

N. S. Chant, L. Rees, and P. G. Roos
University of Maryland, College Park, Maryland 20740

F. E. Bertrand, E. E. Gross, F. E. Obenshain, and T. P. Sjoreen
Oak Ridge National Laboratory, Oak Ridge, Tennessee 37830

G. S. Blanpied, B. M. Preedom, and B. G. Ritchie
University of South Carolina, Columbia, South Carolina 29208
(Received 1 June 1983)

Elastic scattering cross sections for $\pi^{\pm}$ scattering from ^{12}C, ^{13}C, and ^{14}C are presented for pion energies of 65 and 80 MeV and for scattering angles from 20° to 120°. Energy dependent isospin effects are observed. The cross sections were fit with the Kisslinger potential, and the potential strength parameters show an $(N-Z)/A$ dependence similar to that predicted by the impulse approximation at 65 MeV, but not at 80 MeV. Calculations using the Siciliano potential, which contains the explicit isospin dependence of the Lorentz-Lorenz-Ericson-Ericson effect plus isoscalar, isovector, and isotensor terms, indicate the importance and energy dependence of absorption effects. Finally a "model independent" parametrization of the neutron density suggests a neutron excess at the surface of ^{13}C but not ^{14}C.

[NUCLEAR REACTIONS Elastic scattering of 65 and 80 MeV $\pi^{\pm}$ from ^{12}C, ^{13}C, and ^{14}C. Angular distributions: $20° < \theta_{lab} < 120°$. Isospin dependence of optical models.]

I. INTRODUCTION

A great deal of low energy pion-nucleus elastic scattering data has been accumulated.[1-7] For the most part, the data were obtained for positive pions scattering from nuclear targets spanning a wide range of the periodic table in order to map out general features of elastic scattering.

The experiments indicate that in the low energy region, the pion mean free path is long and pions penetrate to the nuclear interior. Optical potentials with no adjustable parameters multiplying the nuclear density ρ yield cross sections which are not in agreement with the data, and terms proportional to ρ^2, such as pion absorption, are important.[8]

Only meager attention has been paid to the isospin dependent part of the pion-nucleus reaction mechanism in the low energy region. This is unfortunate since single and double charge exchange reactions depend specifically on this term. A successful general theory of pion-nucleus reactions should yield cross sections in agreement with elastic scattering as well as charge exchange data.

In the absence of a general theory, phenomenological optical potentials, for example that of Kisslinger, can be used to parametrize elastic scattering data and can be tested on charge exchange data. Existing elastic scattering data[1-7] include nuclei with nonzero isospin. Phenomenological fits to the data[1,2] indicated that the isospin dependence of the best fit optical potential parameters was qualitatively similar to the trends, but not the magnitudes, of an impulse approximation calculation. However, in most cases studied thus far both Z and N were changed. The data herein allow examination of this feature while keeping Z constant.

Another long-standing problem in nuclear physics is the determination of neutron densities. Since at low energies the π^+p and π^-p angular distributions are very different, the scattering of charged pions from isotopes appears to be a fruitful way of attacking the problem. TRIUMF data,[4] in which π^- was scattered from two isotopes of carbon and oxygen, indicated a sensitivity to the neutron radius, but again more data were needed to draw firm conclusions.

In this paper, data are presented for $\pi^{\pm}$ elastic scattering from ^{12}C, ^{13}C, and ^{14}C. The data were obtained for pion energies of 65 and 80 MeV and for scattering angles between 20 and 120 deg. The data are compared with optical potential calculations, the applicability of the impluse approximation is examined, and the importance of absorption terms, Coulomb effects, and neutron distributions are examined.

TABLE I. Elastic scattering cross sections. Relative errors shown are due to statistics. Normalization errors are as follows: 7% (π^+ ^{12}C), 10.5% (π^- 12C); 7% (π^+ ^{13}C), 10.5% (π^- ^{13}C); 14% (π^+ ^{14}C), 16% (π^- ^{14}C).

	80 MeV						65 MeV				
A	$\theta_{c.m.}$ (deg)	$\sigma^+_{c.m.}$ (mb/sr)	$\pm\Delta\sigma^+_{c.m.}$ (mb/sr)	$\sigma^-_{c.m.}$ (mb/sr)	$\pm\Delta\sigma^-_{c.m.}$ (mb/sr)	A	$\theta_{c.m.}$ (deg)	$\sigma^+_{c.m.}$ (mb/sr)	$\pm\Delta\sigma^+_{c.m.}$ (mb/sr)	$\sigma^-_{c.m.}$ (mb/sr)	$\pm\Delta\sigma^-_{c.m.}$ (mb/sr)
12	20.4	57.4	2.25	158.	6.56	12	20.4	24.1	0.8	126.	4.
	25.5	53.8	2.00	123.	5.16		25.4	24.3	0.8	83.2	2.1
	30.6	45.1	2.35	86.9	4.57		30.5	23.2	0.6	62.9	1.6
	35.6	34.3	1.92	60.3	3.16		35.6	18.2	0.5	40.4	1.0
	40.7	25.5	1.28	41.8	2.44		40.7	13.2	0.3	27.9	0.7
	45.8	15.8	0.64	26.4	1.45		45.7	9.41	0.25	17.3	0.5
	50.9	9.82	0.49	15.8	0.91		50.8	6.08	0.19	11.2	0.3
	55.9	5.65	0.30	8.32	0.51		55.9	3.76	0.13	5.66	0.31
	61.0	3.50	0.21	4.82	0.30		60.9	2.33	0.09	3.22	0.14
	66.0	2.18	0.12	3.36	0.21		65.9	1.70	0.06	2.42	0.10
	71.1	1.91	0.10	3.16	0.18		70.9	1.88	0.07	2.13	0.08
	76.1	1.88	0.09	3.25	0.13		75.9	2.30	0.09	2.69	0.09
	81.1	2.38	0.10	3.60	0.22		80.9	2.90	0.10	3.26	0.09
	86.1	2.66	0.10	3.85	0.20		86.0	3.27	0.12	3.44	0.11
	91.1	2.85	0.11	3.83	0.20		90.0	3.62	0.12	4.08	0.12
	96.1	2.91	0.11	3.56	0.29		96.0	3.87	0.11	4.34	0.12
	101.1	2.68	0.10	3.06	0.16		101.0	3.91	0.10	4.65	0.10
	111.0	1.94	0.09	1.90	0.08		111.0	3.63	0.09	3.78	0.17
	116.0	1.27	0.08	1.30	0.05		115.9			2.99	0.10
	121.0	0.88	0.05	0.84	0.05		120.9	2.55	0.07	2.50	0.09
	125.9	0.72	0.05	0.66	0.04						
13	15.3	66.0	4.44	325.	18.	13	20.3	28.6	0.8	143.	3.9
	20.4	71.3	4.47	220.	9.		25.4	29.6	1.1	99.6	2.9
	25.4	63.0	4.07	157.	7.		30.5	26.4	0.7	67.7	1.8
	30.5	52.2	2.81	107.	5.		35.6	21.3	0.5	45.6	1.2
	35.6	40.5	1.07	75.8	2.94		40.6	15.9	0.4	31.7	0.8
	40.7	27.6	0.69	49.4	1.32		45.7	11.0	0.3	19.0	0.5
	45.7	18.4	0.50	29.0	1.07		50.7	6.58	0.19	10.4	0.3
	50.8	10.6	0.31	16.3	0.49		55.8	4.06	0.12	6.18	0.19
	55.8	6.20	0.19	8.91	0.35		60.8	2.69	0.10	3.49	0.14
	60.9	3.51	0.12	5.14	0.19		65.9	2.11	0.07	2.85	0.11
	65.9	2.50	0.08	3.82	0.14		70.9	2.12	0.07	2.90	0.10
	71.0	2.04	0.05	3.89	0.10		75.9	2.49	0.06	3.68	0.17
	76.0	2.35	0.05	4.54	0.11		80.9	3.12	0.09	4.59	0.12
	81.0	2.64	0.07	4.67	0.12		86.0	3.45	0.09	4.63	0.14
	86.0	2.93	0.07	4.93	0.12		91.0	3.82	0.09	5.24	0.15
	91.0	3.55	0.09	4.80	0.11		96.0	3.99	0.10	4.84	0.13
	96.0	3.36	0.11	4.30	0.11		100.9	3.98	0.10	4.74	0.15
	101.0	2.77	0.11	3.24	0.08		105.9			5.01	0.19
	106.0	2.54	0.10	2.31	0.06		110.9	3.14	0.08	4.0	0.41
	110.0	2.03	0.06	1.44	0.05		115.9			3.81	0.23
	115.9	1.49	0.11	0.94	0.07		120.8	2.65	0.09	2.86	0.24
	120.9	1.11	0.09	0.41	0.04						
	125.8	1.12	0.11	0.24	0.04						
14	20.3	97.8	9.7	190.	8.	14	20.3	31.9	1.7	161.	6.
	25.4	70.7	7.8	145.	5.		25.4	32.2	2.1	120.	7.
	30.5	60.3	3.9	92.5	3.5		30.4	30.0	1.4	77.1	4.5
	35.6	42.4	2.2	65.0	2.1		35.5	23.3	1.2	47.9	2.9
	40.6	25.7	1.5	43.1	1.4		40.6	15.5	0.7	33.1	1.7
	45.7	17.0	0.8	26.6	1.1		45.6	10.7	0.5	19.1	0.9
	50.7	9.30	0.50	12.9	0.5		50.7	6.77	0.31	10.9	0.6
	55.8	5.35	0.25	7.52	0.34		55.7	3.96	0.18		
	60.8	3.06	0.18	4.35	0.28		60.8	2.56	0.13	3.70	0.26
	65.9	2.10	0.12	3.78	0.16		65.8	1.87	0.10	3.42	0.16
	70.9	1.92	0.13	3.57	0.12		70.8	1.83	0.09	3.59	0.18

TABLE I. (*Continued.*)

	80 MeV						65 MeV				
A	$\theta_{c.m.}$ (deg)	$\sigma^{+}_{c.m.}$ (mb/sr)	$\pm\Delta\sigma^{+}_{c.m.}$ (mb/sr)	$\sigma^{-}_{c.m.}$ (mb/sr)	$\pm\Delta\sigma^{-}_{c.m.}$ (mb/sr)	A	$\theta_{c.m.}$ (deg)	$\sigma^{+}_{c.m.}$ (mb/sr)	$\pm\Delta\sigma^{+}_{c.m.}$ (mb/sr)	$\sigma^{-}_{c.m.}$ (mb/sr)	$\pm\Delta\sigma^{-}_{c.m.}$ (mb/sr)
	75.9	2.00	0.13	4.14	0.19		75.9	2.02	0.11	3.89	0.16
	80.9	2.40	0.11	4.13	0.21		80.9	2.34	0.12	5.20	0.19
	86.0	2.60	0.09	3.76	0.18		85.9	2.75	0.12	5.59	0.21
	90.0	2.49	0.10	3.36	0.18		90.9	2.95	0.13	5.84	0.25
	96.0	2.06	0.09	2.75	0.16		95.9	2.82	0.13	5.80	0.24
	100.9	1.54	0.09	1.45	0.13		100.9	2.89	0.13	4.74	0.23
	110.9	0.92	0.06	0.90	0.13		110.8	2.15	0.12	3.02	0.17
	120.8	0.45	0.11	0.37	0.14		120.8	1.26	0.12	1.77	0.16

II. EXPERIMENT

The experiment was performed at the low energy pion channel of the Los Alamos Meson Physics Facility using the Bicentennial Spectrometer as described elsewhere.[8] The ^{12}C ($\rho t = 266$ mg/cm^2) and ^{13}C ($\rho t = 576$ mg/cm^2) targets were foils, while the ^{14}C target came in powder form. For the ^{12}C and ^{13}C targets the backgrounds were found to be negligible. For all targets, energy resolution $\lesssim 1$ MeV was achieved and allowed separation of elastic from inelastic scattering.

The ^{14}C powder was contained in a stainless steel container, which was the source of significant background. Thus, empty container data were taken at each scattering angle. In addition, a ^{12}C contamination of $(21.7 \pm 1.7)\%$ (Ref. 9) was used to measure the thickness of the target by comparing the excitation of the 4.44 MeV state of ^{12}C from the contamination with the excitation of the same state from the foil ^{12}C target. The ^{14}C target thickness, thus determined, is $\rho t = (0.107 \pm 0.012)$ g/cm^2.

In order to obtain elastic scattering cross sections from ^{14}C, it was necessary to subtract the contribution due to scattering from the ^{12}C contamination. Since ^{12}C elastic scattering cross sections were measured under the same conditions, such a subtraction could be directly made.

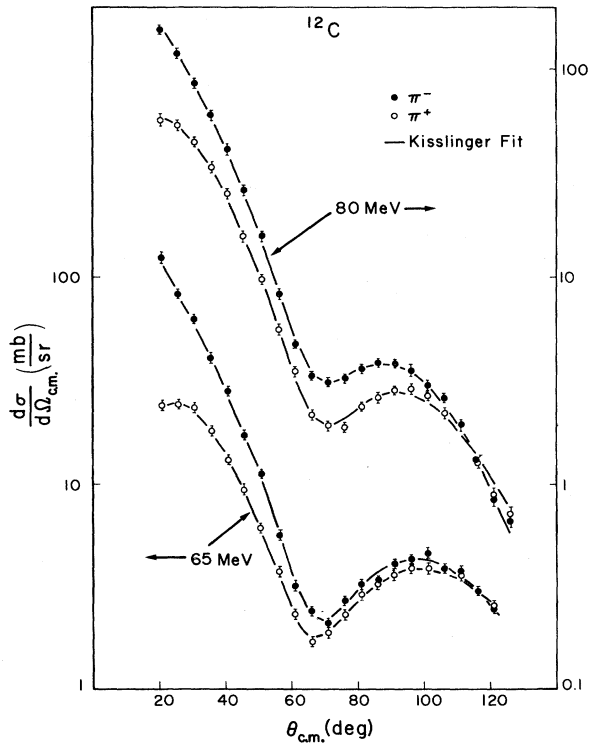

FIG. 1. Center of mass elastic cross sections for $^{12}C(\pi^{\pm},\pi^{\pm})^{12}C$ versus center of mass angle. The solid curves are best fits to the data for a Kisslinger potential.

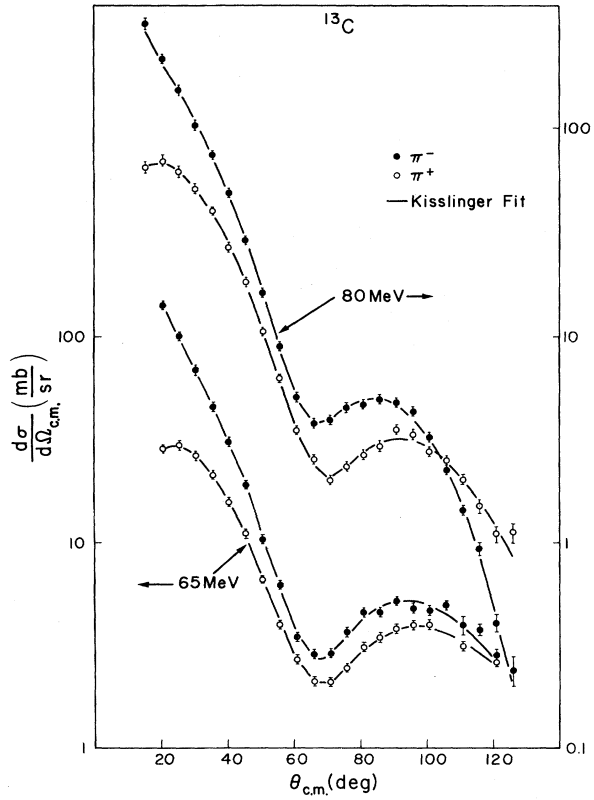

FIG. 2. Center of mass elastic cross sections for $^{13}C(\pi^{\pm},\pi^{\pm})^{13}C$ versus center of mass angle. The solid curves are best fits to the data for a Kisslinger potential.

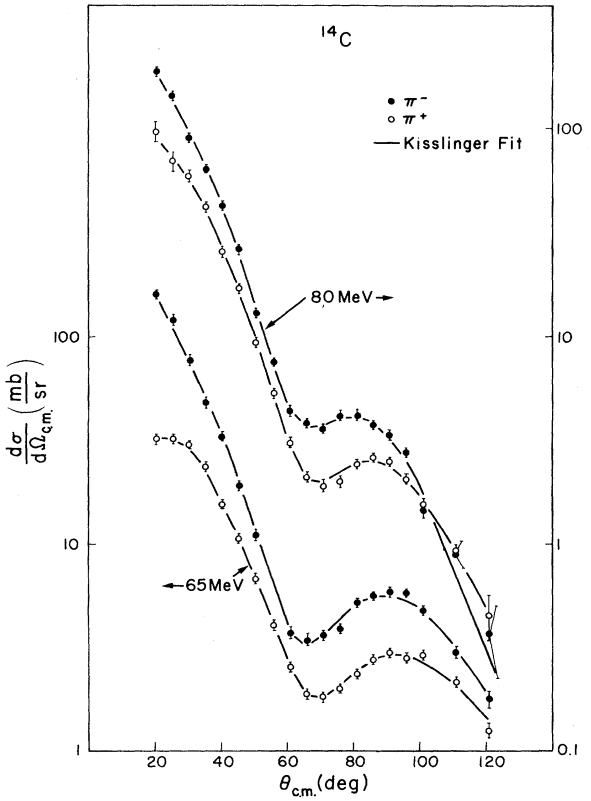

FIG. 3. Center of mass elastic cross sections for $^{14}C(\pi^{\pm},\pi^{\pm})^{14}C$ versus center of mass angle. The solid curves are best fits to the data for a Kisslinger potential.

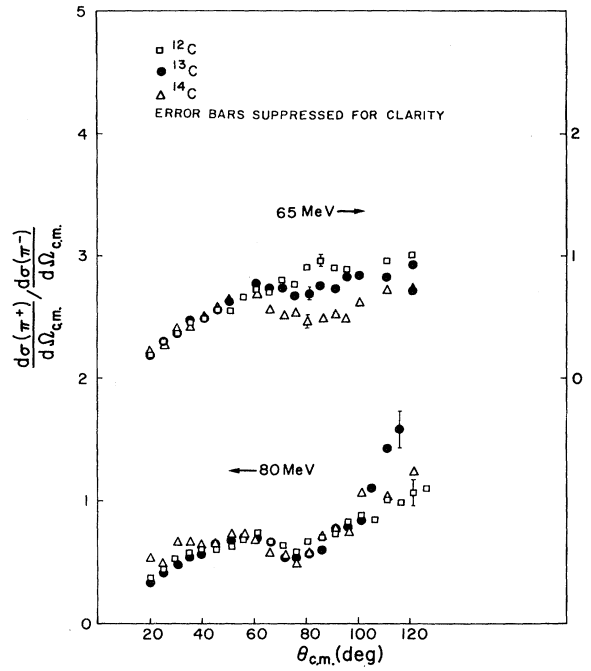

FIG. 4. Ratio of $d\sigma_{\pi^+}/d\sigma_{\pi^-}$ for ^{12}C, ^{13}C, ^{14}C versus center of mass angle.

The 80 MeV ^{12}C data have been reported elsewhere.[6]

Absolute normalizations of the (π^+,π^+) cross sections were obtained by measuring π^+p elastic scattering cross sections and using the published values to calibrate a relative monitor as described in Ref. 8. No adequate values for π^-p elastic scattering exist in the literature. As a result, we determined that the π^- beam spot was the same as the π^+ beam spot when using reversed polarity with the same currents in the beam transport magnets and used the same calibration of the relative monitor as in the π^+ case. The normalization errors in the π^- cross sections were arbitrarily increased as indicated in Table I to account for small differences in geometry.

III. RESULTS

The cross sections are tabulated in Table I and plotted in Figs. 1–3. The errors shown are due to statistics. The cross sections are larger at forward angles for 80 MeV, but fall more rapidly at backward angles, indicating the earlier onset of the first diffraction minimum.

Specific isospin effects are observed. At 80 MeV, $X \equiv d\sigma(\pi^+)/d\sigma(\pi^-)$ becomes greater than 1 for ^{13}C and ^{14}C at smaller angles than for ^{12}C. This feature is also

TABLE II. Best fit Kisslinger strength parameters

E_π (MeV)	Q	A	C (fm)	Reb_0 (fm^3)	Imb_0 (fm^3)	Reb_1 (fm^3)	Imb_1 (fm^3)	χ^2/n_D
80	+	12	2.53±0.06	−1.90±0.20	−0.96±0.19	6.26±0.09	1.96±0.21	32/17
	−		2.60±0.03	−2.07±0.16	−1.54±0.09	6.50±0.08	2.08±0.07	12/17
	+	13	2.51±0.04	−1.65±0.11	−0.99±0.13	5.98±0.06	1.82±0.09	45/18
	−		2.70±0.03	−1.56±0.11	−1.93±0.17	7.35±0.07	2.62±0.08	21/18
	+	14	2.69±0.05	−1.88±0.18	−0.90±0.11	6.68±0.26	3.40±0.56	13/14
	−		2.60±0.02	−2.89±0.31	−0.42±0.11	9.05±0.39	3.65±0.30	27/14
65	+	12	2.59±0.02	−2.79±0.09	−0.65±0.09	6.61±0.08	1.40±0.12	17/14
	−		2.57±0.02	−3.04±0.31	−1.05±0.11	6.54±0.11	1.49±0.43	43/16
	+	13	2.65±0.02	−2.68±0.08	−0.65±0.03	6.45±0.07	1.40±0.11	16/14
	−		2.70±0.02	−3.62±0.36	−1.18±0.12	6.83±0.09	1.27±0.36	47/16
	+	14	2.81±0.03	−2.58±0.14	−0.67±0.06	6.32±0.13	1.70±0.25	9/14
	−		2.87±0.04	−3.60±0.36	−1.62±0.12	7.43±0.14	2.06±0.42	23/13

shown in Fig. 4. Also, the position of the first maximum in the cross section for π^- as compared with π^+ occurs at more forward angles for ^{13}C and ^{14}C.

At 65 MeV, the large angle behavior of the ratio X is reversed. In the region between the first minimum and first maximum, a dramatic decrease in the ratio with increasing isospin occurs. This feature is shown more clearly in Fig. 4. Also, there is little difference in the position of the first maximum for $d\sigma(\pi^-)$ vs $d\sigma(\pi^+)$ for any of the carbon isotopes, although the position of the first maximum occurs at larger angles as compared with the 80 MeV data. This latter observation indicates that the diffraction minimum will occur at larger angles for lower energies, as expected.

IV. ANALYSIS

A. Phenomenological fits

The data were analyzed using optical potentials. In the first instance, the cross sections were fit with the phenomenological Kisslinger optical potential,

$$V(r) = -k^2 b_0 \rho(r) + b_1 \vec{\nabla} \cdot \rho(r) \vec{\nabla} ,$$

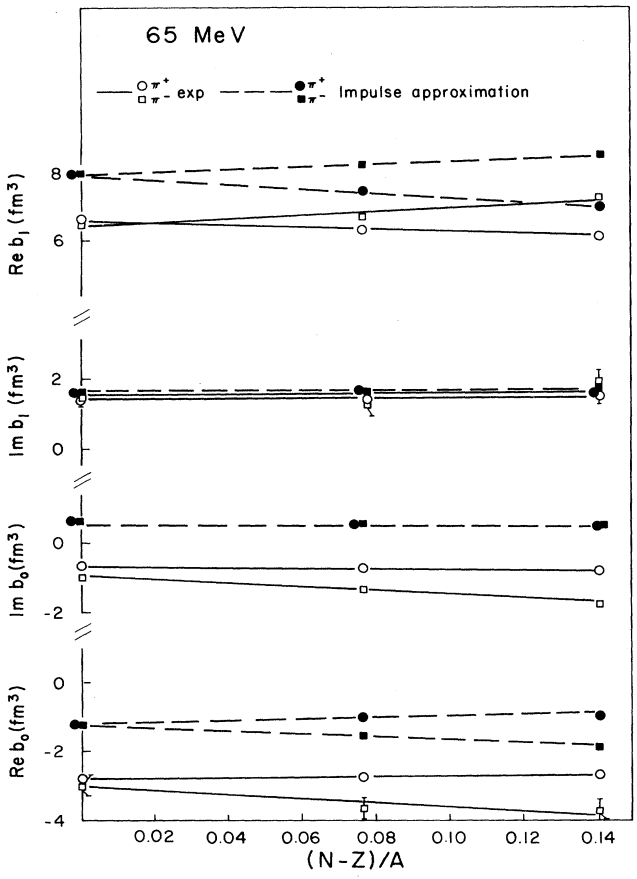

FIG. 5. Best fit and impulse approximation Kisslinger potential parameters and matter radius versus $(N-Z)/A$ for 65 MeV pions.

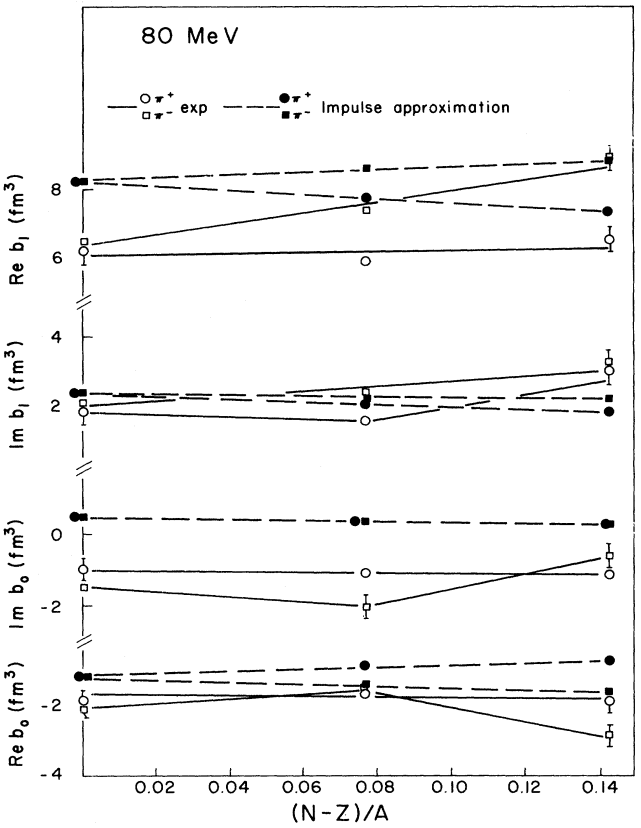

FIG. 6. Best fit and impulse approximation Kisslinger potential parameters and matter radius versus $(N-Z)/A$ for 80 MeV pions.

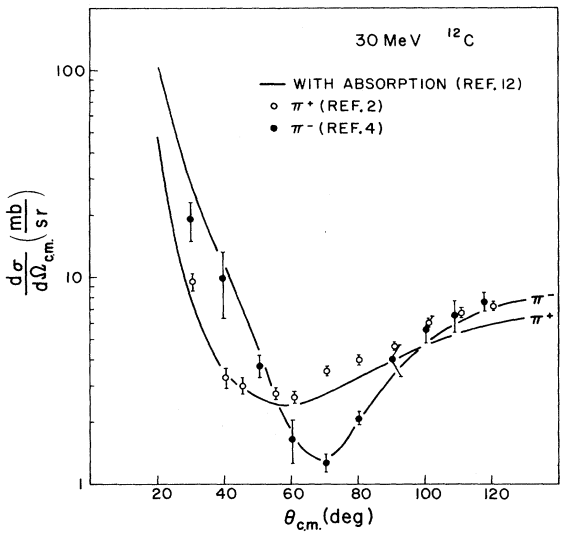

FIG. 7. Center of mass cross sections for $^{12}C(\pi^{\pm},\pi^{\pm})^{12}C$ versus center of mass angle. The solid curves are calculations with the Siciliano potential (see text). The data are from Ref. 2 (π^+) and Ref. 4 (π^-).

where k is the pion-nucleus center of mass wave number. This potential is nonlocal and first order in the nuclear density,

$$\rho(r) \propto \{1+\exp[(r-c/a]\}^{-1},$$

where $a=0.37$ fm. The potential strength parameters b_0, b_1 and the matter radius c (nominally 2.5 fm for ^{12}C) were allowed to vary to obtain a best fit to the cross sections.

The best fit parameters obtained are tabulated in Table II and the cross sections predicted with these parameters are plotted as solid curves in Figs. 1–3. One should note that the parameters are all correlated. Fixing one parameter will change the others, and also the size of the errors.

The potential strength parameters are plotted versus $(N-Z)/A$ in Figs. 5 and 6. Also plotted in Figs. 5 and 6 are the potential strength parameters obtained from an impulse approximation calculation[10] using the latest πN phase shifts.[11] At 65 MeV, there is remarkable agreement in the trends of the fit parameters as compared with the trends of the impulse approximation parameters, although the absolute magnitudes for all parameters, aside from Imb_1, are not in agreement. Also, an increase in the matter radius with increasing isospin appears called for. At 80 MeV, the trends between fitted and impulse approximation parameters are no longer in agreement, which suggests a complicated energy dependence for the isospin part of the Kisslinger potential.

B. Second order effects

Siciliano[12] has developed an optical potential with isoscalar, isovector, and isotensor parts. The potential includes the explicit isospin dependence of the Lorentz-Lorenz-Ericson-Ericson (LLEE) effect which enters to all orders in the nuclear density ρ. Other than the LLEE parameter, there are no adjustable parameters to first order in ρ, while absorption terms proportional to ρ^2 are chosen phenomenologically. In this paper, these parameters have

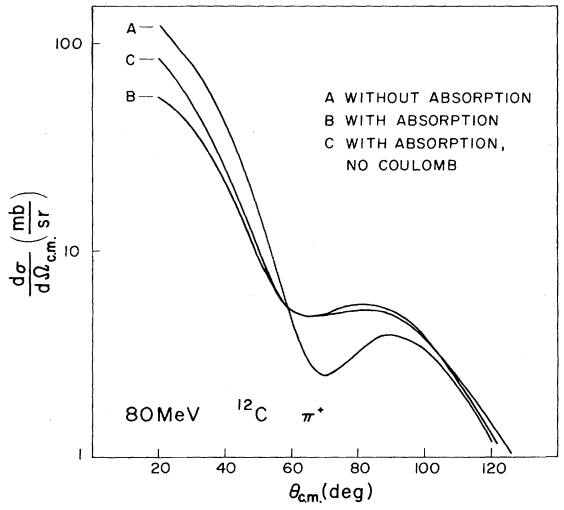

FIG. 8. Calculation of the 80 MeV ^{12}C(π^+,π^+)^{12}C reaction using the Siciliano potential. Curve A excludes absorption. Curve B includes absorption. Curve C is like curve B, but Coulomb terms have been removed.

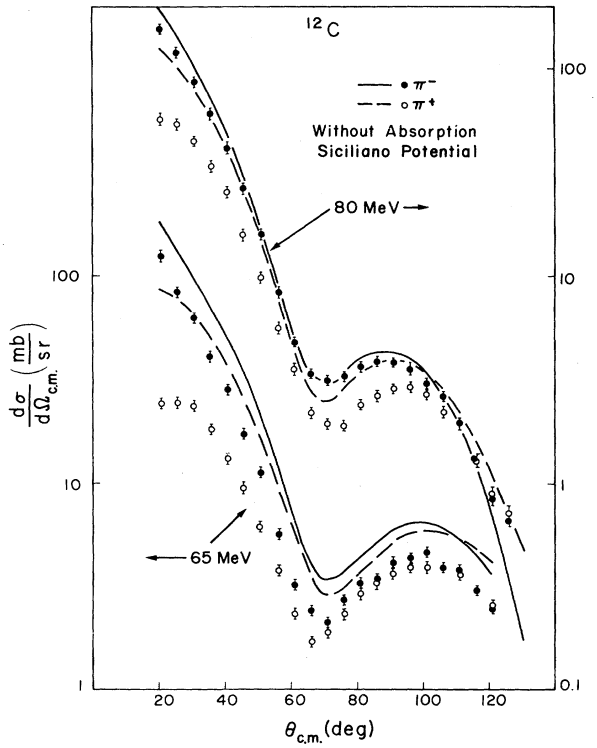

FIG. 9. Center of mass cross sections for ^{12}C($\pi^\pm$,$\pi^\pm$)^{12}C versus center of mass angle. The curves are calculations with the Siciliano potential excluding absorption.

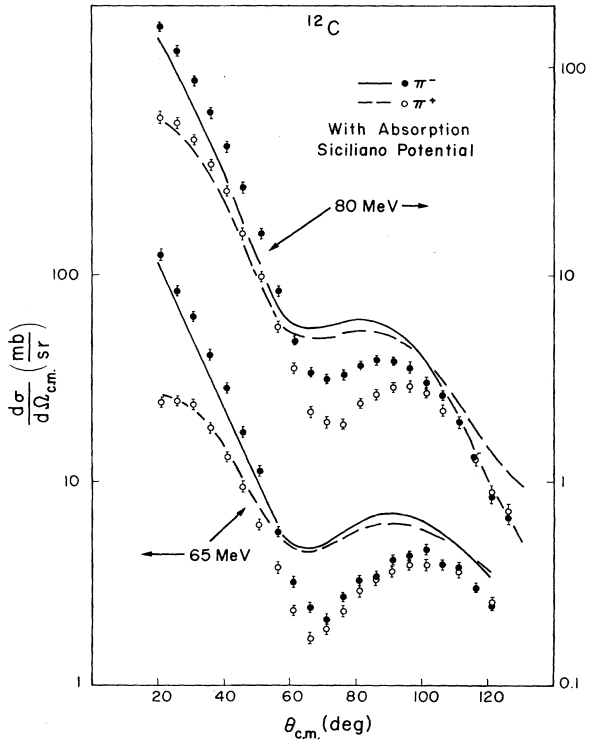

FIG. 10. Center of mass cross sections for ^{12}C($\pi^\pm$,$\pi^\pm$)^{12}C versus center of mass angle. The curves are calculations with the Siciliano potential including absorption.

been taken from pionic atom data. The calculated cross sections reproduce the 30 MeV $\pi^{\pm}$ ^{12}C elastic scattering data very well, as seen in Fig. 7. Without absorption terms the calculation widely disagrees with the 30 MeV data. This potential has been used to calculate elastic scattering cross sections for $\pi^{\pm}$ from ^{12}C and ^{14}C at 65 and 80 MeV.

In Fig. 8, the calculation for 80 MeV π^{+} elastic scattering from ^{12}C is shown to illustrate typical effects. Curve *A* is obtained by neglecting absorption, curve *B* includes absorption, and curve *C* is similar to curve *B* except that the Coulomb interaction has been removed. Coulomb effects are seen to be small except at very forward angles. The major difference in the cross sections is due to inclusion of absorption terms, which tend to fill in the minimum.

In Figs. 9 and 10, calculations without and with absorption are compared with the 65 and 80 MeV $\pi^{\pm}$ ^{12}C elastic scattering data. For 80 MeV, the π^{-} cross section is in fortuitous agreement with the calculation that excludes absorption, while the calculation with absorption gives agreement with the data only at forward angles. The above remarks also hold for scattering from ^{14}C, as illustrated in Figs. 11 and 12.

It is apparent that absorption effects are energy dependent, and the parameters determined from pionic atom data cannot be used at these energies. Microscopic calculations of these quantities are desired. At this point, however, fits of the Siciliano potential to elastic scattering cross sections of pions from isotopes are still useful. Such a potential, because of its isovector and isotensor terms, appears appropriate to analyze charge exchange data. Data for the elastic scattering of pions from isotopes should constrain this potential sufficiently to test its applicability with regard to charge exchange reactions.

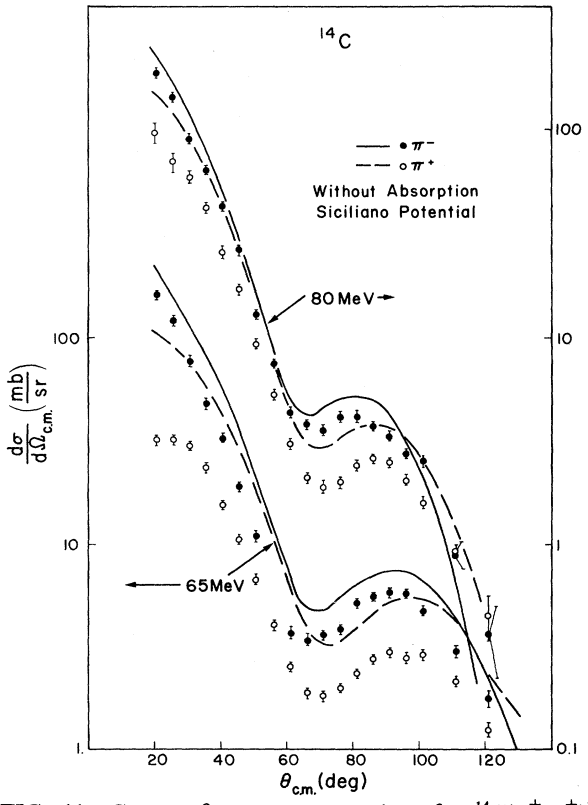

FIG. 11. Center of mass cross sections for ^{14}C($\pi^{\pm}$,$\pi^{\pm}$)^{14}C versus center of mass angle in degrees. The curves are calculations with the Siciliano potential excluding absorption.

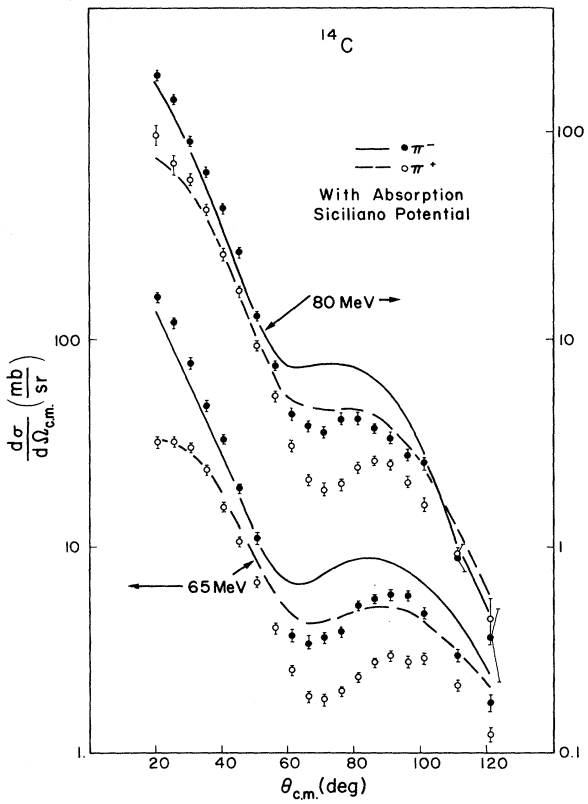

FIG. 12. Center of mass cross sections for ^{14}C($\pi^{\pm}$,$\pi^{\pm}$)^{14}C versus center of mass angle in degrees. The curves are calculations with the Siciliano potential including absorption.

C. Neutron densities

A long-standing problem in nuclear physics has been the determination of neutron densities, ρ_n. Low energy elastic scattering of both π^{+} and π^{-} from isotopes appears to be a fruitful reaction from which this quantity may be determined. This is because the point Coulomb part of the interaction is kept fixed, the π^{+}p and π^{-}p angular distributions are vastly different at low energies, and the pion mean free path in nuclear matter is large at low energies.

Information on the neutron densities can be obtained from optical potential analyses of elastic scattering data. When the parameters of a potential are determined from fits to the data for a nucleus whose neutron density is assumed known, then use of these parameters in analyzing data for neighboring nuclei may allow determination of the neutron densities of the latter. This method is most suitable for studies of isotopes. The present data were analyzed by Friedman[13] using a technique which was most successful in analyses of elastic scattering of α parti-

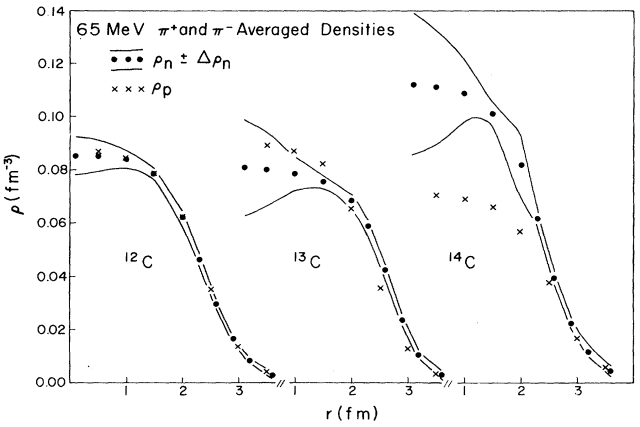

FIG. 13. Neutron densities averaged from the Friedman analysis (see the text) of the π^+ and π^- 65 MeV data. The lines indicate the extent of the errors obtained in evaluating the density. Also shown ($\times$) are the proton densities, taken as two parameter Fermi functions.

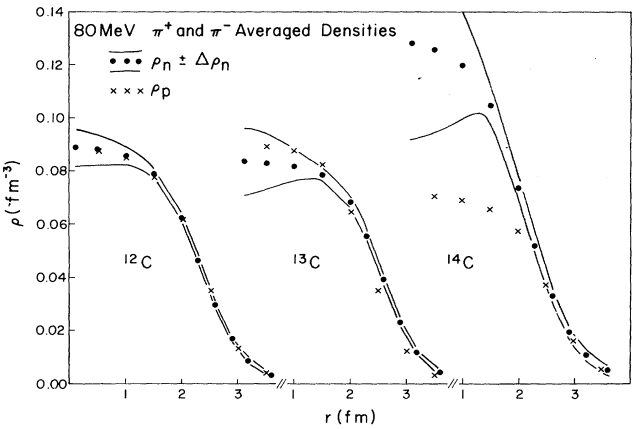

FIG. 14. Neutron densities averaged from the Friedman analysis (see the text) of the π^+ and π^- 80 MeV data. The lines indicate the extent of the errors obtained in evaluating the density. Also shown ($\times$) are the proton densities, taken as two parameter Fermi functions.

cles.[14] Fits were made to the 65 and 80 MeV ^{12}C data with the Ericson-Ericson[15] potential without the LLEE effect, but with angle transformation terms. In this case, ρ_n is assumed the same as ρ_p, for which a two parameter Fermi function normalized to Z is used. This density cannot exhibit any shell model features but reproduces the density at the nuclear surface very well.

The potential parameters obtained by fitting the $\pi^{\pm}$ ^{12}C data are isospin corrected for ^{13}C and ^{14}C using parameters from fits to pionic atom data. In view of previous discussion, use of pionic atom data is subject to question. For ^{13}C and ^{14}C, ρ_n is expanded in a Fourier-Bessel (FB) series as outlined in Ref. 14, and the coefficients of the expansion are varied to provide a best fit to the elastic scattering data. It is to this extent that ρ_n is "model independent." As a test this is also done for ^{12}C and the assumed ρ_n is indeed found, within the errors. By using FB densities and not Fermi functions, more realistic estimates of the uncertainties in ρ_n are obtained.

Good fits to the 80 MeV ^{12}C data were found in which the parameters for π^+ and π^- scattering were the same. A similar situation was observed at 65 MeV. The neutron densities, normalized to N, which are obtained have large errors in the region of the nuclear interior. However, at the nuclear surface, $r \gtrsim 2.0$ fm, the errors are reasonably small and allow some conclusions to be drawn.

The densities obtained from the π^- data are consistent with those obtained from the π^+ data. The average density is contained within the band of solid lines in Figs. 13 and 14. For ^{14}C, ρ_n and ρ_p are the same in the surface region, but for ^{13}C is an excess of neutrons at the nuclear surface. This is reasonable, as the binding energies of the last one or two neutrons in ^{13}C and ^{14}C are 4.95 and 8.18 MeV, respectively. Errors in all the parameters are correlated and thus it was not possible to extract accurate values for the root-mean-square (rms) neutron radius, contrary to the situation with alpha particles.[14]

V. CONCLUSIONS

Energy dependent isospin effects in scattering of $\pi^{\pm}$ from ^{12}C, ^{13}C, and ^{14}C at 65 and 80 MeV have been observed. When the cross sections are fit with a Kisslinger potential, the potential strength parameters show the same trends as those indicated by an impulse approximation calculation at 65 MeV, but not at 80 MeV. Comparison of the cross sections with those calculated using the Siciliano potential, which contains LLEE, isoscalar, isovector, and isotensor terms shows the importance and the energy dependence of absorption effects. A "model-independent" parametrization of the neutron density indicates an excess of neutrons relative to protons at the nuclear surface of ^{13}C but not ^{14}C.

ACKNOWLEDGMENTS

The authors thank the Los Alamos National Laboratory staff for their technical assistance; E. Siciliano and E. Friedman for stimulating discussions and allowing use of their calculations in this manuscript; and R. R. Johnson for providing cross sections from the TRIUMF work. This work was supported by the National Science Foundation (Virginia Polytechnic Institute and State University, University of Maryland, and University of South Carolina) and the Department of Energy [LAMPF and ORNL (under Contract W-7405-eng-26 with the Union Carbide Corporation)].

[1]M. Blecher, K. Gotow, D. Jenkins, F. Milder, F. E. Bertrand, T. P. Cleary, E. E. Gross, C. A. Ludemann, M. A. Moinester, R. L. Burman, M. Hamm, R. P. Redwine, M. Yates-Williams, S. Dam, C. W. Darden III, R. D. Edge, D. J. Malbrough, T. Marks, and B. M. Preedom, Phys. Rev. C 20, 1884 (1979).

[2]B. M. Preedom, S. H. Dam. C. W. Darden III, R. D. Edge, D. J. Malbrough, T. Marks, R. L. Burman, M. Hamm, M. A. Moinester, R. P. Redwine, M. A. Yates, F. E. Bertrand, T. P. Cleary, E. E. Gross, N. W. Hill, C. A. Ludemann, M. Blecher, K. Gotow, D. Jenkins, and F. Milder, Phys. Rev. C 23, 1134 (1981).

[3]S. A. Dytman, J. F. Amman, P. D. Barnes, J. N. Craig, K. G. R. Doss, R. A. Eisenstein, J. D. Sherman, W. R. Wharton, G. R. Burleson, S. L. Verbeck, R. J. Peterson, and H. A. Thiessen, Phys. Rev. C 19, 971 (1979).

[4]R. R. Johnson, T. Masterson, B. Bassalleck, W. Gyles, T. Marks, K. L. Erdman, A. W. Thomas, D. R. Gill, E. Rost, J. J. Kraushaar, J. Alster, C. Sabev, and J. Arvieux, Phys. Rev. Lett. 43, 844 (1979); R. R. Johnson, private communication.

[5]S. H. Dam, R. D. Edge, B. M. Preedom, M. Hamm, R. L. Burman, R. Carlini, R. P. Redwine, M. A. Yates, M. Blecher, K. Gotow, F. E. Bertrand, E. E. Gross, and M. A. Moinester, Phys. Rev. C 25, 2574 (1982).

[6]M. Blecher, R. Auble, F. E. Bertrand, W. Bertozzi, G. Blanpied, R. L. Burman, R. Carlini, S. Dam, W. Gaskin, K. Gotow, E. E. Gross, M. V. Hynes, M. A. Kovash, M. J. Leitch, F. E. Obenshain, B. M. Preedom, R. P. Redwine, B. G. Ritchie, V. Sandberg, and J. Wu, in *Proceedings of the Ninth International Conference on High Energy Physics and Nuclear Structure, Versailles, 1981,* edited by P. Catillon, R. Radvanyi, and M. Porneuf (North-Holland, Amsterdam, 1982).

[7]F. E. Obenshain, F. E. Bertrand, M. Blecher, R. L. Burman, R. D. Edge, K. Gotow, E. E. Gross, M. Hamm, M. J. Leitch, M. A. Moinester, B. M. Preedom, R. P. Redwine, and J. R. Wu, in *Proceedings of the Ninth International Conference on High Energy Physics and Nuclear Structure, Versailles, 1981,* edited by P. Catillon, R. Radvanyi, and M. Porneuf (North-Holland, Amsterdam, 1982).

[8]M. Blecher, K. Gotow, R. Ng, R. L. Burman, R. Carlini, S. Dam, M. V. Hynes, M. J. Leitch, V. Sandberg, R. Auble, F. E. Bertrand, E. E. Gross, F. E. Obenshain, J. Wu, G. S. Blanpied, B. M. Preedom, B. G. Ritchie, W. Bertozzi, M. A. Kovash, and R. P. Redwine, Phys. Rev. C 25, 2554 (1982).

[9]H. Baer, private communication.

[10]E. H. Auerbach, D. M. Fleming, and M. M. Sternheim, Phys. Rev. 162, 1683 (1967).

[11]SAID—Scattering Analysis Interactive Dial In, available from R. A. Arndt and L. D. Roper, Virginia Polytechnic Institute and State University, Blacksburg, VA 24061.

[12]E. Siciliano, private communication. For general information see also M. B. Johnson and E. R. Siciliano, Phys. Rev. C 27, 730 (1983); 27, 1647 (1983).

[13]E. Friedman, private communication, and (unpublished).

[14]E. Friedman, H. T. Gils, H. Rebel, and Z. Majka, Phys. Rev. Lett. 41, 1220 (1978); H. T. Gils, E. Friedman, Z. Majka, and H. Rebel, Phys. Rev. C 21, 1245 (1980); E. Friedman, H. T. Gils, and H. Rebel, *ibid.* 25, 1551 (1982).

[15]M. Ericson and T. E. O. Ericson, Ann. Phys. (N.Y.) 36, 323 (1965).